Original Article

Optimized low-dose positron emission tomography/computed tomography schemes in pediatric tumor patients: a randomized clinical trial

Songke Yu[#], Zhongjie Qian[#], Hongli Liu[#], Rongqin Fan, Xueqin Long, Bo Li, Qian Zhang, Yumei Wang, Lin Cao, Rui Zhou, Dingyou Hou, Daiqiang Gao, Lisheng Liu, Xiaoliang Chen

Department of Nuclear Medicine, Chongqing University Cancer Hospital, Chongqing, China

Contributions: (I) Conception and design: S Yu, Z Qian, R Fan, X Long; (II) Administrative support: S Yu, H Liu, Q Zhang, X Chen; (III) Provision of study materials or patients: Z Qian, R Fan, X Long, B Li, Q Zhang, R Zhou, D Hou, D Gao; (IV) Collection and assembly of data: Z Qian, R Fan, X Long ; (V) Data analysis and interpretation: Z Qian, R Fan, X Long, Y Wang, L Cao, L Liu, X Chen; (VI) Manuscript writing: All authors; (VII) Final approval of manuscript: All authors.

[#]These authors contributed equally to this work and should be considered as co-first authors.

Correspondence to: Songke Yu. Department of Nuclear Medicine, Chongqing University Cancer Hospital, Chongqing, China.
Email: cquchnmysk@cqu.edu.cn.

Background: It's clinically relevant to reduce the radiation dose to children while ensuring their positron emission tomography/computed tomography (PET/CT) image quality. The optimal protocol for whole-body PET/CT imaging in children (non-model) has been less studied. In this study, we investigated the optimal protocol for PET/CT imaging of pediatric oncology by analyzing the radiation dose and image quality in18F-fluoro-2-deoxy-D-glucose (^{18}F-FDG) PET/CT imaging of children with oncology.

Methods: One hundred children with tumors who underwent ^{18}F-FDG PET/CT were included. CT grouping: randomly divided into 18 groups A–R according to the combination of three parameters: tube voltage (80/120 kV), automatic milliamp range (20–39/40–59/60–80 mA), and noise index (NI) (8/12/14). PET grouping: randomly divided into 9 groups a–i according to the combination of two parameters: the pharmaceuticals injection dose (0.08/0.12/0.15 mCi/kg) and time per bed (120/150/180 s). The effective radiation dose (ED) was calculated separately for each group and the image quality of CT and PET was evaluated subjectively using standard deviation (SD) and coefficient of variation (CV) objective evaluation and 5-point evaluation method, respectively.

Results: Ninety-seven images in CT and 57 images in PET were included. The best quality of CT images was in group K (120 kV/40–59 mA/8); there are 9 groups had good image quality and lower dose length product (DLP) than group K (SD ±10), while the difference in DLP between groups was large. The Kruskal-Wallis (K-W) test showed that the difference in image quality between the 9 groups was not statistically significant. The best PET image quality was in group i [0.15 (mCi/kg)/180 s]; there are four groups had good image quality and lower ED_{PET} than group i (CV ±3.5%), while the difference in ED_{PET} between groups was large (4.4–6.5 mSv), and the K-W test showed that the difference in image quality between the four groups was not statistically significant (P>0.05), with the lowest ED_{PET} being in the g group.

Conclusions: The optimal protocols for CT scanning and PET imaging in this experiment were group H (80 kV/40–59 mA/14) and group g [0.08 (mCi/kg)/180 s], respectively.

Trial Registration: Chinese Clinical Trial Registry ChiCTR2200061386.

Keywords: Pediatric tumor; ^{18}F-fluoro-2-deoxy-D-glucose positron emission tomography/computed tomography (^{18}F-FDG PET/CT); image quality; coefficient of variation (CV); radiation dose

Submitted Jul 05, 2022. Accepted for publication Sep 14, 2022.
doi: 10.21037/tp-22-371
View this article at: https://dx.doi.org/10.21037/tp-22-371

Introduction

The morbidity and mortality rates of childhood malignant tumors are gradually rising. It is estimated that by 2050, there will be 13.7 million children with malignant tumors worldwide, and about 11.1 million children will die of cancer (1). In China, malignant tumors are the second leading cause of death in children (2). The early and accurate diagnosis of childhood malignancies followed by effective treatment can improve patient prognosis (3). Recent studies have shown that ^{18}F-fluoro-2-deoxy-D-glucose positron emission tomography/computed tomography (^{18}F-FDG-PET/CT) is highly valuable for the imaging of active lesions, the detection of metastases in lymph nodes, liver, bone, and other sites, the assessment of bone marrow involvement, prognostic prediction, and response assessment in pediatric tumor patients (4-12). According to the newly revised "International Neuroblastoma Response Criteria" (13,14), PET/CT has higher sensitivity and specificity in the detection of active neuroblastoma and ganglioneuroblastoma and the assessment of tumor metastasis. Thus, PET/CT is an ideal examination method for tumors in children.

PET/CT is highly recognized for its accuracy in the detection, characterization, and treatment monitoring of tumors, as it provides valuable diagnostic information that may not be readily available using other imaging techniques. The medical benefits of PET/CT outweigh the risks in most cases; however, caution should be exercised when exposing children to ionizing radiation (13,14). We must assess the PET/CT radiation dose received by patients, especially in the pediatric populations, as children are more sensitive to radiation than adults due to their rapid rate of cell division. Exposure to the same radiation dose may produce higher random levels of ionizing radiation in children (15). The risk of cancer in infants is more than 10 times that of adults under the same radiation dose (16). Gonadal radiations cause greater genetic damage to children than adults (17). Compared to adult CT, pediatric CT may significantly increase the estimated risk of death from cancer (18). The lifetime attributable risks of all cancer morbidity and mortality in 10-year-old children (males and females) were almost 5.29 and 3.16 times that of 70-year-old adults (men and women), and these risks were even greater for younger children (19). Thus, it is of clinical significance to reduce the radiation dose while ensuring the quality of PET/CT images in children.

To date, a recent study has focused on the estimation of effective doses (EDs) and the assessment of radiation risks in adults (20). However, few studies have investigated the image quality and radiation dose of whole-body ^{18}F-FDG PET/CT in children, and some studies were performed using models of childhood diseases. Fahey *et al.* studied the dose of CT in pediatric PET examinations and found that the use of multiple sequential acquisitions was effective in reducing patient dose (21); Guo *et al.* performed PET/CT whole-body imaging in 36 pediatric patients and found that it was feasible to shorten the acquisition time and reduce the amount of tracer injection, and that the reduction in acquisition time from 180 to 120 s did not lose diagnostic quality, and that weight The dose could be reduced by 22.22% at 30 kg or less, but the small sample size in this study made it difficult to apply the final results widely (22); Zhao *et al.* retrospectively analyzed PET/CT data from 33 pediatric patients and found good image scores for ^{18}F-FDG doses administered in the range of 0.37–1.85 MBq/kg, although this study was The higher dose images that had been acquired were reconstructed with reduced photon counts to obtain similar low-dose graphics, so the final dose was not necessarily accurate (23). Routinely, the higher the CT scan parameters used the better the CT image quality, and the higher the radiopharmaceutical dose the better the PET image quality, but it is clearly undesirable to simply improve image quality while ignoring radiation dose. Based on the above clinical study design idea, in this study we analyzed the data of 100 children who underwent whole-body ^{18}F-FDG PET/CT at our center to explore the optimal low-dose PET/CT scheme in terms of image quality and radiation dose. We present the following article in accordance with the CONSORT reporting checklist (available at https://tp.amegroups.com/article/view/10.21037/tp-22-371/rc).

Methods

Study design

This prospective, completely randomized study was approved by the Ethics Committee of Chongqing University Cancer Hospital (No. CZLS2022022-A). All the subjects and their families signed the informed consent documents. This study was conducted in accordance with the Declaration of Helsinki (as revised in 2013).

The study sought to address the issue of reducing the radiation dose to children with tumors while ensuring the quality of their PET/CT images. Children with tumors

Table 1 CT group I (with a tube voltage of 80 kV)

Noise index	Auto mA (mA)		
	20–39	40–59	60–80
8	A	B	C
12	D	E	F
14	G	H	I

A–I are 9 groups composed of different tube current and noise index at 80 kV. CT, computed tomography.

Table 2 CT group II (with a tube voltage of 120 kV)

Noise index	Auto mA (mA)		
	20–39	40–59	60–80
8	J	K	L
12	M	N	O
14	P	Q	R

J–R are 9 groups composed of different tube current and noise index at 120 kV. CT, computed tomography.

were randomly assigned to CT and PET groups with different combinations of parameters, and the EDs of CT and PET were calculated separately for each group and the quality of CT and PET images of all children was evaluated according to the subject-client evaluation method, using noise [standard deviation (SD)] for CT images and coefficient of variation (CV) for PET images. Scatter plots of the data and comparisons between groups were performed using statistical and graphing software based on the objective and subjective evaluation indexes. The balance between image quality and radiation dose was analyzed to obtain a better image quality while minimizing the radiation dose to the child.

The sample size estimation procedures

The sample size of this study had incomplete case information, bias in basic information, small lesions, liver metastases, uncooperative children, excessive blood glucose, and inaccurate region of interest (ROI) outlining, which resulted in poor quality CT images and unusable PET images found to have large differences in standard uptake value (SUV) values or CV values. Kang *et al.* retrospectively included 20 patients over 8 years (6). Yağci-Küpeli *et al.* retrospectively studied data from 94 pediatric patients (range, 1–18 years) over 4 years (9). Sung *et al.* retrospectively studied 55 children (10). Nowadays, most studies have too low data volume or large range, in this paper, 94 cases of CT images and 57 cases of PET images were included to ensure the data volume while keeping the range at 5–9 years.

Subjects

A total of 100 children with tumors (comprising 53 males and 47 females, aged 5–9 years) who underwent ^{18}F-FDG PET/CT at the Department of Nuclear Medicine of Chongqing University Cancer Hospital from May 2021 to April 2022 were included in this study. To be eligible for inclusion in this study, the children had to meet the following inclusion criteria: (I) be aged 5–9 years old, 97.5–110 cm in height, and 14.5–18.5 kg in weight; and (II) whose liver and gallbladder are normal, with no tumor involvement. The children were excluded from the study if they met any of the following exclusion criteria: (I) had diabetes or fasting blood glucose ≥11.1 mmol/L; and/or (II) were unable to cooperate during the PET/CT.

Equipment and methods

The GE Discovery 710 PET/CT scanner was used. CT scanning was performed 1st according to the grouping parameters, followed by PET acquisition.

Grouping

(I) CT grouping: the tube voltage set for the 2 groups was 80 and 120 kV, the range of auto mA set for the 3 groups was 20–39, 40–59, and 60–80 mA, and the noise index (NI) set for the 3 groups was 8, 12, and 14. The combinations of these 3 grouping results yielded 18 groups (designated as groups A to R) (see *Tables 1*,*2*). The children were randomly divided into these 18 groups, which comprised 5–6 children per group.

(II) PET grouping: the ^{18}F-FDG injection dose was divided into 3 groups of 0.08, 0.12, and 0.15 mCi/kg, and the acquisition time per bed was set to 120, 150, and 180 s. The combinations of these 3 injection groups and 3 acquisition time groups yielded 9 groups (designated as groups a to i) (see *Table 3*). The children were randomly divided into these 9 groups, which comprised 11–12 children per group.

Table 3 PET grouping

Acquisition time per bed (s)	Dose (mCi/kg)		
	0.08	0.12	0.15
120	a	b	c
150	d	e	f
180	g	h	i

a–i are 9 groups composed of injection doses and acquisition time per bed. PET, positron emission tomography.

The corresponding injection dose was injected, and abdominal PET images were collected according to the acquisition time.

Preparation before scans

The subjects were fasted and abstained from sugar for 6 hours before the PET/CT scans. Their body height and weight were measured, and their medical histories were taken. During the waiting period, examination, sedation, and removal of metal foreign bodies, the children were accompanied by family members. Sedatives were used as necessary to relieve anxiety. The patients were asked to avoid wearing metal objects. Family members were required to wait with their children.

CT scan

In each CT group, the corresponding grouping parameters were applied; however, the following parameters remained the same: helical scan; smart mA mode; rotation speed: w0.6 s/R (seco nd/circle); detector width: 40 mm; slice thickness: 3.75 mm; and pitch and speed: 0.984:1 (mm/rot). The reconstructed slice thickness was 1.25 mm, and the adaptive statistical iterative reconstruction was 40%. All the images were sent to the AW4.6 post-processing workstation.

PET acquisition

In each PET group, the corresponding grouping parameters were applied; however, the following parameters remained the same: 3-dimesional acquisitions were performed for 5 beds, and 30% overlapped. Image reconstruction was performed using an ordered subset expectation maximization algorithm plus time-of-flight technology, and the number of iterations was 2. All the images were sent to the AW4.6 post-processing workstation.

Image and data processing

Calculation of radiation dose

The following formula was used to calculate the CT dose: $ED_{CT} = k \times DLP = k \times CTDI_{VOL} \times L$, where k is the weighting factor [mSv/(mGy·cm)], and the weighting factor of the ED_{CT} in the trunk of children aged 5–10 years is 0.019 (24), $CTDI_{VOL}$ (mGy) represents the volume CT dose index of the multi-slice spiral CT scans, L represents the scanning length of different parts of the human body along the Z axis, and DLP (mGy·cm) represents the dose length product and is calculated using the following formula: $DLP = CTDI_{vol} \times L$ (where L is the direct read on PET/CT equipment).

The following formula was used to calculate the PET dose: $ED_{PET} = A \times W_{FDG}$, where ED_{PET} is the radiation dose (mSv) from PET, A is the activity (MBq) of the radiopharmaceutical ^{18}F-FDG injected into the patient, and W_{FDG} (mSv/MBq) is the dose conversion factor of activity and the ED for children of different age groups recommended by the "International Commission on Radiological Protection Publication 80", in which the conversion factor of 0.056 for children aged 5–10 years is selected (25).

The following formula was used to calculate the total radiation dose: $ED_{TOTAL} = ED_{CT} + ED_{PET}$ (ED_{TOTAL} is the total ED from the PET/CT scans).

Region of interest

ROI selection and delineation were conducted on the GE AW4.6 workstation. The CT and PET cross-sections were selected to delineate the ROI of the image background. Each ROI had the same size (e.g., *Figure 1A*,*1B*). The SD of the CT values in the ROI was measured on the CT image (*Figure 1A*), and the mean and SD of the SUV in the ROI were measured on the PET image (*Figure 1B*). During the delineation, the liver parenchyma was selected and the hepatic hilum, blood vessels, gallbladder, and other areas were avoided. In this study, one plane was selected every 3–6 slices, and 2–3 ROIs were delineated per plane. The final data of a specific case was the average of the measured data.

The ROI was independently delineated by 2 experienced technicians, and the obtained data were analyzed for consistency.

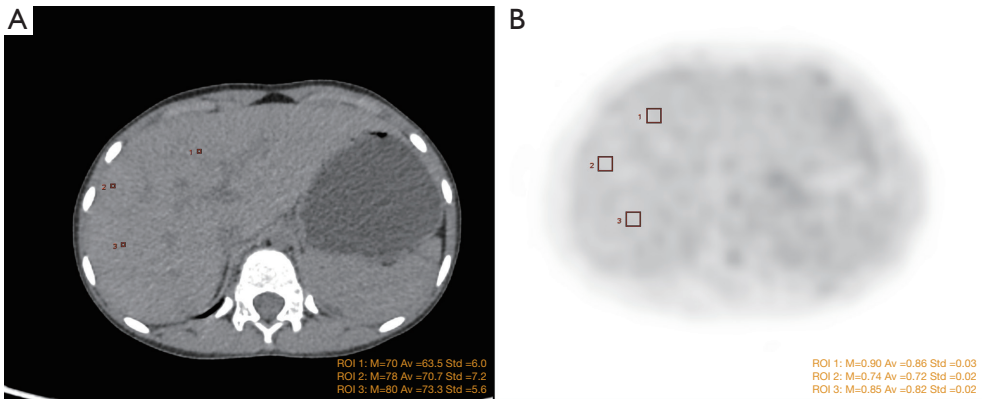

Figure 1 ROI selection and delineation in liver parenchyma: (A) on a CT cross-section; (B) on a PET cross-section. ROI, region of interest; CT, computed tomography; PET, positron emission tomography; M, max; Av, average; Std, standard deviation.

Image quality evaluation

Subjective evaluation

The quality of the CT and PET images were evaluated on the same Picture Archiving and Communication Systems by two senior nuclear medicine physicians who conducted a visual grading characteristic analysis. For the CT images, on the abdominal window, a 5-point scoring system was used for the evaluation according to: (I) the contrast of various abdominal organs, blood vessels, bile ducts, and lymph nodes; (II) the degree of lesion display; and (III) noise and artifacts. For the PET images, a 5-point scoring system was used for the evaluation according to: (I) the contrast of various abdominal organs/tissues and lymph nodes; and (II) noise and artifacts. The detailed evaluation criteria are as follows:

- 5 points—on the image, the tissue structure is very clear, with good contrast, fine texture, and little noise; it fully meets the requirements of clinical diagnosis;
- 4 points—on the image, the tissue structure is clear, with relatively fine texture and relatively little noise; it meets the requirements of clinical diagnosis;
- 3 points—on the image, the texture is fair, with relatively much noise and missing of some tissue structures; it basically meets the requirements of clinical diagnosis;
- 2 points—on the image, there is much noise and poor texture, with poorly displayed tissue structures; it cannot meet the requirements of clinical diagnosis;
- 1 point—on the image, there is a large number of noise and extremely poor texture, without the display of tissue structures; it has no diagnostic value at all;
- Images with a score of ≥3 points were considered to meet the diagnostic requirements (see *Figure 2A*,*2B*), and the scoring results of the two physicians were analyzed for consistency.

Objective evaluation

(I) CT image quality evaluation: noise is used as an objective index for CT image quality evaluation. Noise refers to unnecessary or redundant interference information existing in image data and is represented by the SD of the CT values in the ROI. The ROIs were drawn at the center level of each major abdominal organ and tissue, and the SDs under different scanning conditions were recorded. The larger the SD, the larger image noise and the worse the image quality.

(II) PET image quality evaluation: the CV was used as an objective indicator of PET image quality. The CV refers to the ratio of the SD to the mean. The following formula was used to calculate the CV: $CV = BG_{SD}/BG_{MEAN} \times 100\%$, where BG_{MEAN} is the mean SUV of the background ROI, and BG_{SD} is the SD of SUV of the background ROI. The CV can eliminate the effects of different units and/or means on the comparison of the degree of variation in 2 or more data. In general, the smaller the CV, the better the image quality.

Statistical analysis

The ROI data delineated by the two technicians and the

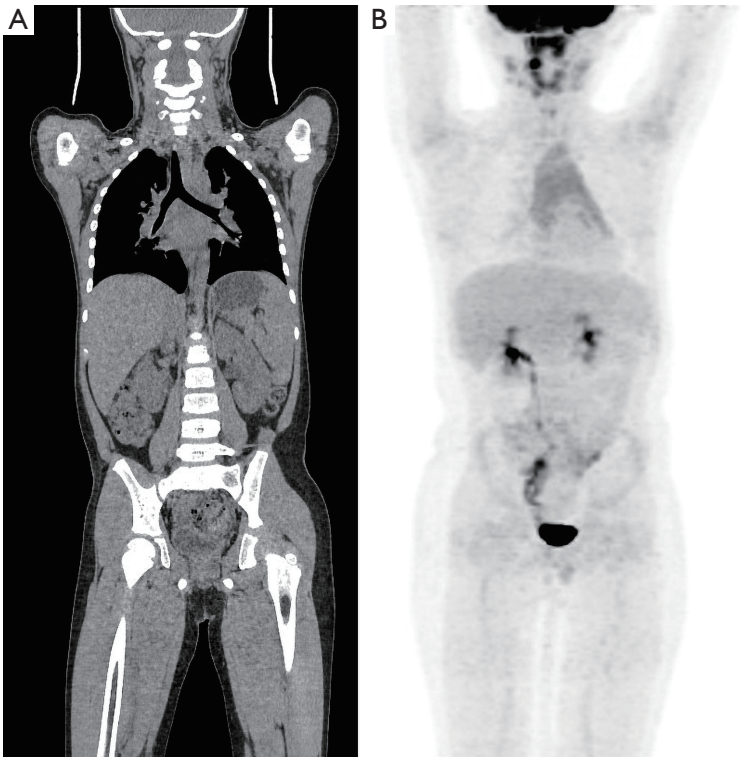

Figure 2 Whole-body PET/CT: (A) coronal CT image; (B) coronal PET image. CT, computed tomography; PET, positron emission tomography.

subjective evaluation of image quality by the two physicians were analyzed for consistency. The EDs of the CT groups A–R and the EDs of the PET groups a–i were calculated. The image quality scores and SD values of the CT groups A–R, the image quality scores and CV values of the PET groups a–i were obtained through the subjective and objective evaluation of the image quality. The data were summarized, analyzed, and visualized using Stata 17.0, GraphPad prism, Origin 8.5, and other statistical and graphing software. Comparisons of the normally distributed data among multiple groups were based on a one-way analysis of variance. The data without normal distribution were analyzed by the rank-sum test. The optimal scheme was selected based on the subjects with the lowest radiation dose in the imaging groups with relatively good CT or PET image quality (subjective score >3 points).

Results

From May 2021 to April 2022, 108 children underwent PET/CT, 8 were excluded before the trial, 1 had fasting glucose ≥11.1 mmol/L, and 7 were unable to cooperate to complete PET/CT imaging. One hundred children were randomly assigned to each trial group. After the study, 94 children with CT images and 57 children with PET images were obtained by excluding children who did not meet the test requirements according to the study protocol. The Consolidated Standards of Reporting Trials (CONSORT) diagram is shown in *Figure 3*. Baseline characteristics table of children is shown in *Table 4*. The ROI measurement results of the two technicians were consistent (P>0.05). The subjective evaluation results of the two senior physicians were likewise consistent (P>0.05).

Data calculation results

The mean value of the SD and DLP measurements and the ED were calculated for each CT group. The maximum value of the SD was 17.502 (in group A) and the minimum value was 7.089 (in group K); the maximum value of the DLP was 270.778 mGy (in group L) and the minimum value was 42.584 mGy (in group G); and the maximum

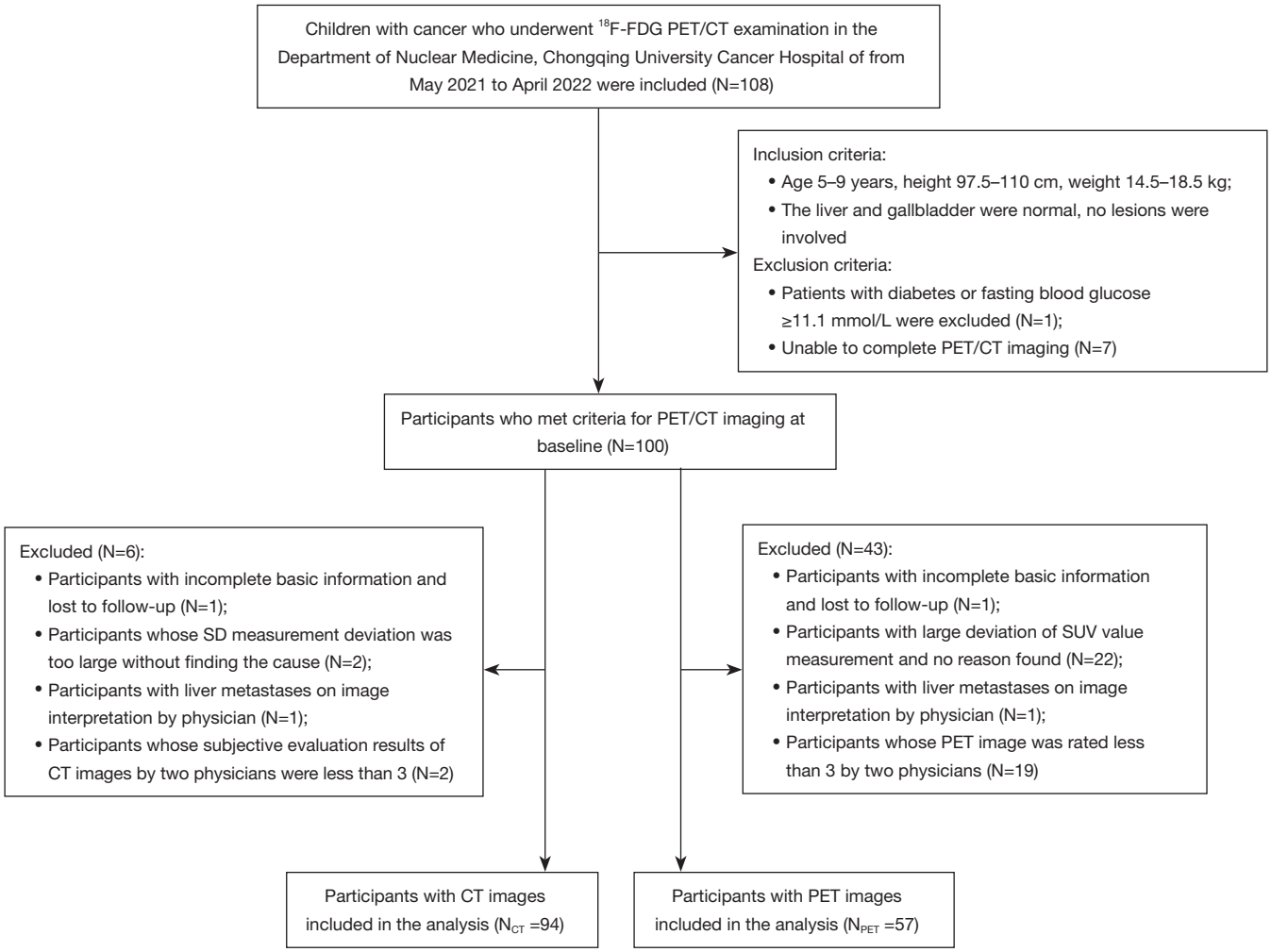

Figure 3 The CONSORT flow diagram of study participants. N_{CT} represents the cases out of 100 subjects that met the inclusion criteria for CT images, and N_{PET} represents the cases out of 100 subjects that met the inclusion criteria for PET images. ^{18}F-FDG PET/CT, ^{18}F-fluoro-2-deoxy-D-glucose positron emission tomography/computed tomography; SUV, standard uptake value; CONSORT, Consolidated Standards of Reporting Trials.

value of the ED was 5.145 mSv (in group L) and the minimum value was 0.809 mSv (in group G). The SD values were relatively close (range, 9.216–11.409 mSv) among 9 of the CT groups (i.e., groups C, E, F, H, I, J, M, P, and Q). The mean value of the CV measurements and the calculated ED were calculated for each PET group, and the maximum value of the CV was 4.934% (in group a) and the minimum value was 2.868% (in group i). The maximum value of the ED was 10.609 mSv (in group b) and the minimum value was 2.538 mSv (in group g). The CV values were relatively close (range, 3.564–3.948%) among 4 of the PET groups (i.e., groups e, f, g, and h).

Scatter plots and statistical analysis results

CT

With the DLP as the horizontal axis and the SD value as the vertical axis, the mean values of all the CT groups were plotted in a scatter diagram (see *Figure 4*), which indicated that the point with the best image quality was point K, which corresponded to group K, whose SD value was 7.089 mGy and whose DLP value was 227.180 mGy. The subjective evaluation showed that 9 groups (i.e., groups C, E, F, H, I, J, M, P, and Q) with SD values of around 10 scored >3 points, in which the image quality was good and the DLP was lower than that of group K. However, there

Table 4 Baseline characteristics table of children

Baseline characteristic	Value (N=100, N_{CT} =94, N_{PET} =57)
Average age (years old)	6.5
≥5, <6	49
≥6, <8	29
≥8, <9	22
Gender	
Male	53
Female	47
Average height (cm)	102.17
Average weight (kg)	17.26
CT scan parameters	
Tube voltage (kV)	
80	46
120	54
Auto tube current (mA)	
20–39	26
40–59	43
60–80	31
Noise index	
8	31
12	35
14	34
PET parameters	
Average injected dose (mCi)	2.433
Injected dose per weight (mCi/kg)	
0.08	33
0.12	37
0.15	30
Acquisition time per bed (s)	
120	35
150	33
180	32
Pathological types of lesions	
Neuroblastoma	39
Lymphoma	24
Rhabdomyosarcoma	12
Other diseases	25

CT, computed tomography; PET, positron emission tomography.

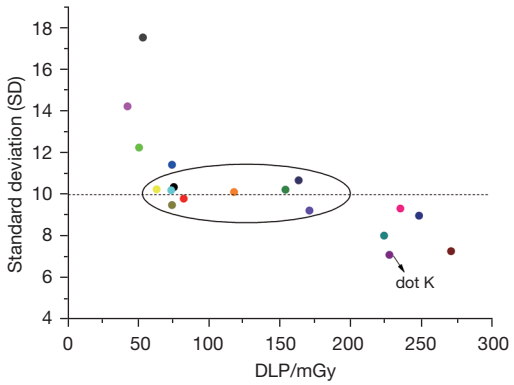

Figure 4 A scatter diagram of the mean values of all the CT groups (with the DLP as the horizontal axis and the SD value as the vertical axis). CT, computed tomography; DLP, dose length product; SD, standard deviation.

was a large difference in the DLPs among these groups (range, 63–171 mGy). Among these 9 groups, the DLP value was the largest in group Q (170.826 mGy) and the smallest in group H (63.106 mGy). These 9 groups were set as group CT 1–9 and imported into the Stata 17.0 software. After testing, not all the groups had normal distribution. Thus, the Kruskal-Wallis (K-W) test was used to compare the SD values among these groups. The Stata results were as follows: chi2(8) =9.510 and probability (Prob) =0.3011; and chi2(8) with ties =9.511 and Prob =0.3010. Thus, the differences among these 9 groups were not statistically significant (P>0.05; see *Figure 5*).

PET

With the ED_{PET} as the horizontal axis and the CV value as the vertical axis, the mean values of all PET groups were plotted in a scatter diagram (see *Figure 6*), which indicated that the point with the best image quality was point i, which corresponded to group i, whose CV value was 2.868% and whose ED_{PET} value was 8.168 mGy. The subjective evaluation showed that 4 groups (i.e., groups e, f, g, and h) with CV values of around 3.75% had a mean score >3 points, in which the image quality was good, and the ED_{PET} was lower than that of group i. However, there was a large difference in the ED_{PET} among these groups (range, 2.538–6.5 mGy). Among these 4 groups, the ED_{PET} value was the largest in group f (6.500 mGy) and the smallest in group g (2.538 mGy). These 9 groups were set as group PET 1–4 and imported into the Stata 17.0 software. After testing, not all the groups had a normal distribution. Thus,

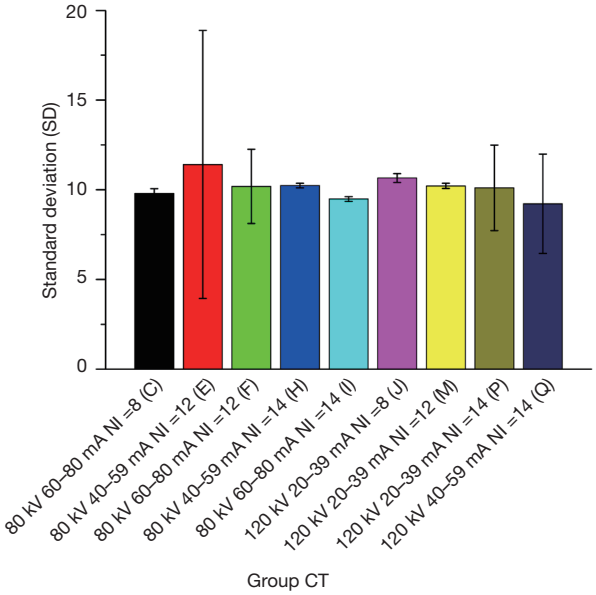

Figure 5 Kruskal-Wallis equality-of-population rank tests for the CT groups. CT, computed tomography; NI, noise index.

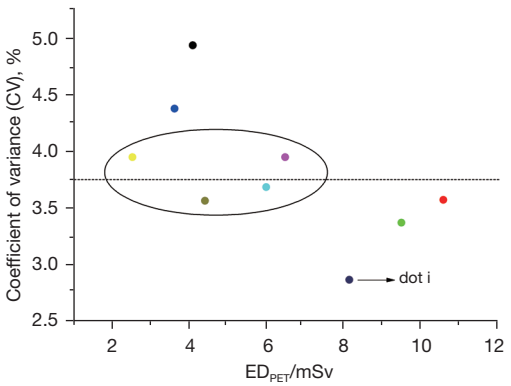

Figure 6 A scatter diagram of the mean values of all the PET groups (with the ED_{PET} as the horizontal axis and the CV value as the vertical axis). PET, positron emission tomography; CV, coefficient of variation; ED_{PET}, effective dose of PET.

the K-W test was used to compare the CV values among these groups. The Stata results were as follows: chi2(3) =3.197 and Prob =0.3623; and chi2(3) with ties =3.197 and Prob =0.3623. Thus, the differences among these 4 groups were not statistically significant (P>0.05; see *Figure* 7).

Discussion

During PET/CT examinations, patients are inevitably

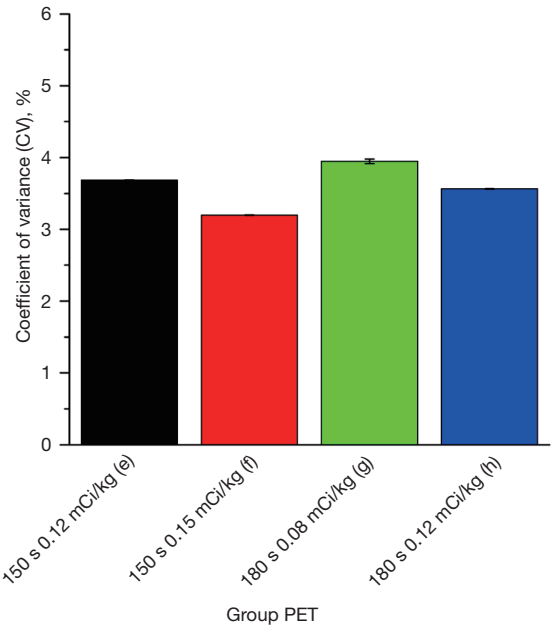

Figure 7 Kruskal-Wallis equality-of-population rank tests for the PET groups. PET, positron emission tomography.

exposed to a certain amount of ionizing radiation. The radiation dose is far lower than the national standard; however, children are more susceptible to ionizing radiation injury because they are in a period of vigorous and quick growth and development. Additionally, the latency periods of malignancies are longer in children (at least 10 years for most solid cancers) than adults (26). Thus, when PET/CT is performed in children, efforts should be made to ensure high-image quality while minimizing the radiation dose (23,27).

In the current study, detailed low-dose CT and PET imaging schemes were formulated. After comparisons among multiple groups, group H (80 kV/40–59 mA/14) had the optimal CT scanning scheme, with a SD value of 10.233 and an ED_{CT} of 1.199 mSv, and group g [0.08 (mCi/kg)/180 s] had the optimal PET scheme, with a CV value of 3.948% and an ED_{PET} of 2.538 mSv. Additionally, as shown in the DLP-SD scatter diagram and the ED_{PET}-CV scatter diagram (*Figures 4*,*5*), the points with the best image quality were points K and i, which corresponded to group K (120 kV/40–59 mA/8), SD value 7.089 mSv, and ED_{CT} 4.316 mSv) and group i [0.15 (mCi/kg)/180 s, CV value: 2.868%, and ED_{PET}: 8.168 mSv], respectively. However, due to the relatively high ED values in group K and group i, the therapeutic

regimens in groups H and K and in groups g and i should be selected in an individualized manner. For example, the regimes in groups H and g, which require a lower radiation dose, may be selected if: (I) PET/CT scans will be performed repeatedly within a short period; (II) the patient has received radiation therapy multiple times in a short period of time; (III) the patient is young; and (IV) there is a relatively low requirement for image quality. Conversely, the therapeutic regimes in groups K and i can be considered if the clinical requirements for image quality are high.

Our present study was limited by its small sample size, which may have affected the accuracy of the results. Future studies should focus on the comparisons of different imaging protocols for different tumor types, the use of multi-organ EDs in phantoms, the monitoring of the EDs of whole-process PET/CT (including repeated imaging) in children, and the rationalization and optimization of therapeutic regimes.

Conclusions

In relation to the ^{18}F-FDG PET/CT of children with tumors, group H (80 kV/40–59 mA/14) had the optimal CT scan scheme and group g [0.08 (mCi/kg)/180 s] had the optimal PET imaging scheme. The use of these two imaging schemes can ensure good image quality while minimizing the radiation dose received during examinations.

Acknowledgments

We would like to thank the Department of Nuclear Medicine of Chongqing University Cancer Hospital, the Children's Radiation Therapy Center of Chongqing University Cancer Hospital, the Research and Foreign Affairs Department of Chongqing University Cancer Hospital for their valuable support.

Funding: The study was supported by the Science and Technology Bureau of Shapingba District, Chongqing (project No. Jcd202122).

Footnote

Reporting Checklist: The authors have completed the CONSORT reporting checklist. Available at https://tp.amegroups.com/article/view/10.21037/tp-22-371/rc

Trial Protocol: Available at https://tp.amegroups.com/article/view/10.21037/tp-22-371/tp

Data Sharing Statement: Available at https://tp.amegroups.com/article/view/10.21037/tp-22-371/dss

Conflicts of Interest: All authors have completed the ICMJE uniform disclosure form (available at https://tp.amegroups.com/article/view/10.21037/tp-22-371/coif). The authors have no conflicts of interest to declare.

Ethical Statement: The authors are accountable for all aspects of the work in ensuring that questions related to the accuracy or integrity of any part of the work are appropriately investigated and resolved. This study was approved by the Ethics Committee of Chongqing University Cancer Hospital (ethics number: CZLS2022022-A). All the subjects and their families signed the informed consent documents. This study was conducted in accordance with the Declaration of Helsinki (as revised in 2013).

References

1. Atun R, Bhakta N, Denburg A, et al. Sustainable care for children with cancer: a Lancet Oncology Commission. Lancet Oncol 2020;21:e185-224.
2. Zhou YL, An JL, Tian L, et al. Epidemiological analysis of childhood cancer in China. Chinese Journal of Contemporary Pediatrics 2015;17:649-54.
3. Vali R, Alessio A, Balza R, et al. SNMMI Procedure Standard/EANM Practice Guideline on Pediatric 18F-FDG PET/CT for Oncology 1.0. J Nucl Med 2021;62:99-110.
4. Bar-Sever Z, Biassoni L, Shulkin B, et al. Guidelines on nuclear medicine imaging in neuroblastoma. Eur J Nucl Med Mol Imaging 2018;45:2009-24.
5. Bagatell R, McHugh K, Naranjo A, et al. Assessment of Primary Site Response in Children With High-Risk Neuroblastoma: An International Multicenter Study. J Clin Oncol 2016;34:740-6.
6. Kang SY, Rahim MK, Kim YI, et al. Clinical Significance

of Pretreatment FDG PET/CT in MIBG-Avid Pediatric Neuroblastoma. Nucl Med Mol Imaging 2017;51:154-60.
7. Park JR, Bagatell R, Cohn SL, et al. Revisions to the International Neuroblastoma Response Criteria: A Consensus Statement From the National Cancer Institute Clinical Trials Planning Meeting. J Clin Oncol 2017;35:2580-7.
8. Ishiguchi H, Ito S, Kato K, et al. Diagnostic performance of 18F-FDG PET/CT and whole-body diffusion-weighted imaging with background body suppression (DWIBS) in detection of lymph node and bone metastases from pediatric neuroblastoma. Ann Nucl Med 2018;32:348-62.
9. Yağci-Küpeli B, Koçyiğit-Deveci E, Adamhasan F, et al. The Value of 18F-FDG PET/CT in Detecting Bone Marrow Involvement in Childhood Cancers. J Pediatr Hematol Oncol 2019;41:438-41.
10. Sung AJ, Weiss BD, Sharp SE, et al. Prognostic significance of pretreatment 18F-FDG positron emission tomography/computed tomography in pediatric neuroblastoma. Pediatr Radiol 2021;51:1400-5.
11. Ko KY, Yen RF, Ko CL, et al. Prognostic Value of Interim 18F-DOPA and 18F-FDG PET/CT Findings in Stage 3-4 Pediatric Neuroblastoma. Clin Nucl Med 2022;47:21-5.
12. Geitenbeek RTJ, Martin E, Graven LH, et al. Diagnostic value of 18F-FDG PET-CT in detecting malignant peripheral nerve sheath tumors among adult and pediatric neurofibromatosis type 1 patients. J Neurooncol 2022;156:559-67.
13. Gelfand MJ, Sharp SE, Treves ST, et al. Estimated cumulative radiation dose from PET/CT in children with malignancies. Pediatr Radiol 2010;40:1712-3; author reply 1714-5.
14. Sgouros G, Frey EC, Bolch WE, et al. An approach for balancing diagnostic image quality with cancer risk: application to pediatric diagnostic imaging of 99mTc-dimercaptosuccinic acid. J Nucl Med 2011;52:1923-9.
15. Robbins E. Radiation risks from imaging studies in children with cancer. Pediatr Blood Cancer 2008;51:453-7.
16. Recommendations of the International Commission on Radiological Protection. Annals of the ICRP 1991;21:1-201. Available online: https://journals.sagepub.com/doi/pdf/10.1177/ANIB_21_1-3
17. Ware DE, Huda W, Mergo PJ, et al. Radiation effective doses to patients undergoing abdominal CT examinations. Radiology 1999;210:645-50.
18. Brenner D, Elliston C, Hall E, et al. Estimated risks of radiation-induced fatal cancer from pediatric CT. AJR Am J Roentgenol 2001;176:289-96.
19. Mohammadi N, Akhlaghi P. Evaluation of radiation dose to pediatric models from whole body PET/CT imaging. J Appl Clin Med Phys 2022;23:e13545.
20. Li Y, Jiang L, Wang H, et al. EFFECTIVE RADIATION DOSE OF 18F-FDG PET/CT: HOW MUCH DOES DIAGNOSTIC CT CONTRIBUTE? Radiat Prot Dosimetry 2019;187:183-90.
21. Fahey FH, Goodkind A, MacDougall RD, et al. Operational and Dosimetric Aspects of Pediatric PET/CT. J Nucl Med 2017;58:1360-6.
22. Guo F, Cui J, Zhang H, et al. Parameter optimal selection during pediatric 18F-FDG PET/CT examination. International Journal of Biomedical Engineering 2014;37:299-302.
23. Zhao YM, Li YH, Chen T, et al. Image quality and lesion detectability in low-dose pediatric 18F-FDG scans using total-body PET/CT. Eur J Nucl Med Mol Imaging 2021;48:3378-85.
24. Yue BR, Niu YT. Managing patient dose in multi-detector computed tomography (MDCT). Beijing: People's Military Med Press, 2011.
25. Mattsson S, Johansson L, Leide Svegborn S, et al. Radiation Dose to Patients from Radiopharmaceuticals: a Compendium of Current Information Related to Frequently Used Substances. Ann ICRP 2015;44:7-321.
26. Kornerup JS, Brodin P, Birk Christensen C, et al. Use of PET/CT instead of CT-only when planning for radiation therapy does not notably increase life years lost in children being treated for cancer. Pediatr Radiol 2015;45:570-81.
27. Verhagen MV, Menezes LJ, Neriman D, et al. 18F-FDG PET/MRI for Staging and Interim Response Assessment in Pediatric and Adolescent Hodgkin Lymphoma: A Prospective Study with 18F-FDG PET/CT as the Reference Standard. J Nucl Med 2021;62:1524-30.

(English Language Editor: L. Huleatt)

Cite this article as: Yu S, Qian Z, Liu H, Fan R, Long X, Li B, Zhang Q, Wang Y, Cao L, Zhou R, Hou D, Gao D, Liu L, Chen X. Optimized low-dose positron emission tomography/computed tomography schemes in pediatric tumor patients: a randomized clinical trial. Transl Pediatr 2022;11(9):1510-1520. doi: 10.21037/tp-22-371